<u>Supplementary Material for Nandi et al</u>, "The CSF-1 receptor ligands IL-34 and CSF-1 exhibit distinct developmental brain expression patterns and regulate neural progenitor cell maintenance and maturation"

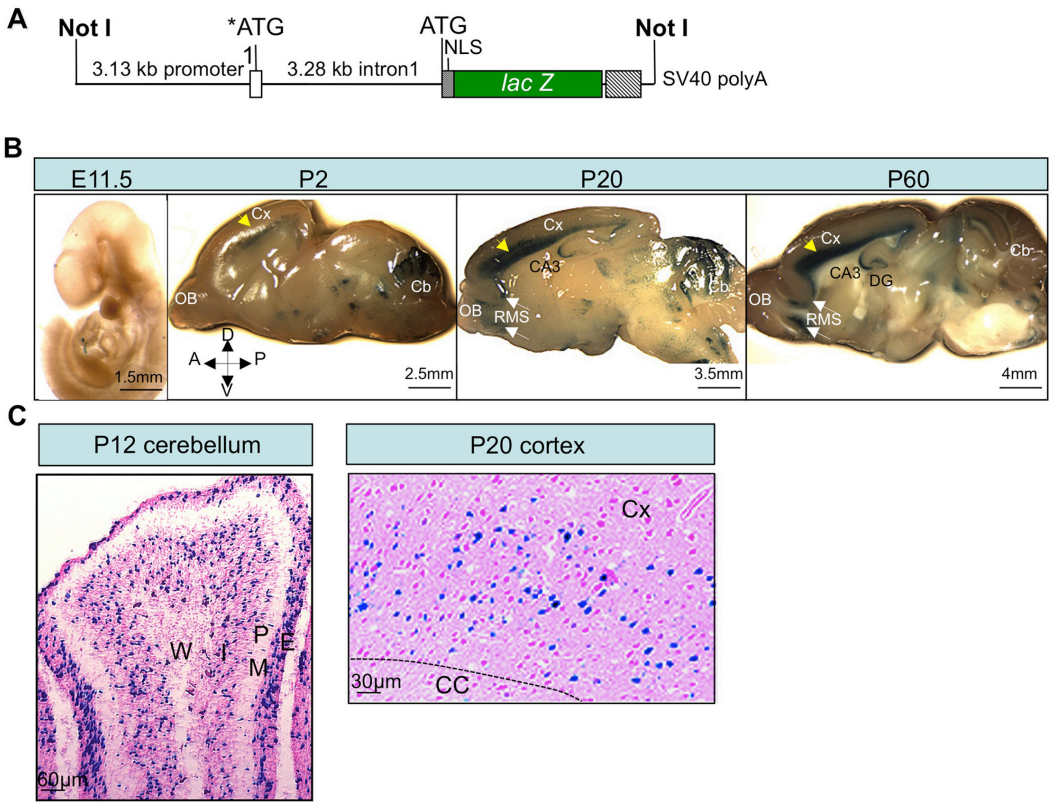

Fig. S1. *Csf1* promoter activity in the developing brain. (A) The *TgZ* transgenic construct. The nuclear localization sequence (NLS)-β-galactosidase (LacZ) coding sequence with a 3' SV40 polyA addition site is driven by the 3.13 Kb CSF-1 promoter and 3.28 Kb first intron fragment. The ATG start codon in exon 1 of the CSF-1 gene was mutated to allow translation initiation from the ATG at the 5' end of the NLS-β-galactosidase coding sequence (Dai et al., 2004; Nandi et al., 2006; Ryan et al., 2001). (B) Sagittal view of LacZ expression by X-gal staining in the embryonic and postnatal CNS. E11.5 whole mount embryos: absence of LacZ expression. Whole-mount and mid-sagittal, postnatal brains: Expression in the deep neocortical layers (P2-P60, yellow arrowheads), the CA3 region (P20, P60), the DG (P60) and the proximity of the RMS (P20, P60, white arrows). Note strong expression patterns in cerebellum at P2 and P20, but not at P60. (C) Left panel: LacZ expression in postnatal tissues: mid-sagittal section depicting cerebellar folium (P12). Right panel: Coronal section showing cerebral cortex (P20); dotted line delineates the border of the corpus callosum with the cortex. W, white matter; I, internal granular layer; P, Purkinje cell layer; M, molecular layer; E, external granular layer; Cx, cortex; OB, olfactory bulb; RMS, rostral migratory stream; DG, dentate gyrus; LV, lateral ventricle; Cb, cerebellum; CC, corpus callosum; A, anterior; P, posterior; D, dorsal; V, ventral.

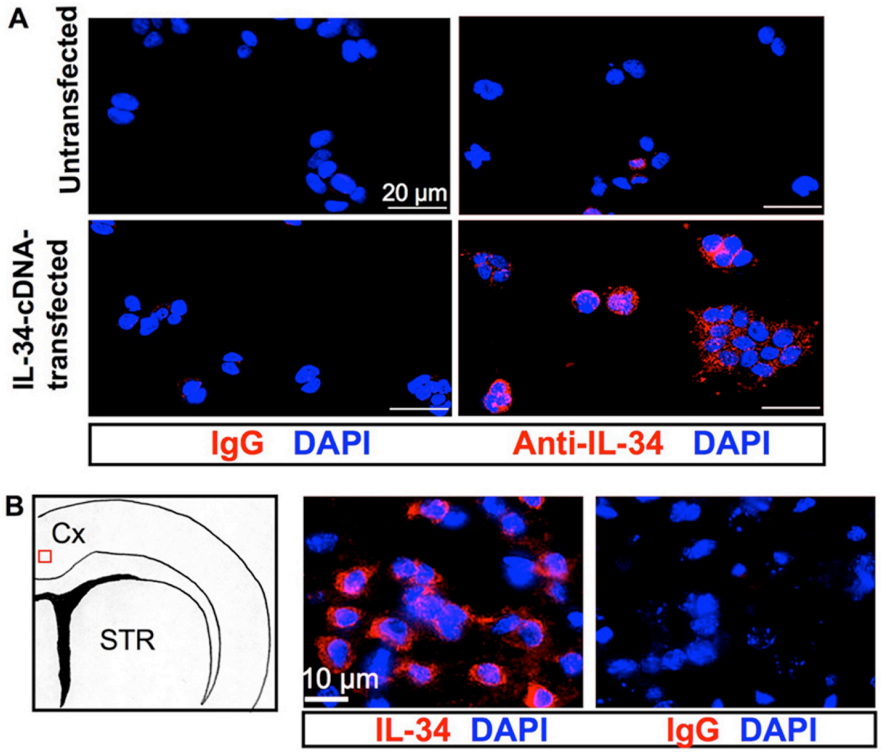

Fig. S2. Specificity of the anti-IL-34 antibody. (A) Immunofluorescence staining of untransfected and mouse IL-34 cDNA-transfected 293T cells with anti-IL-34 antibody or control IgG (red) and DAPI. (B) Immunofluorescence micrography showing staining of postnatal dorsal forebrain as shown in the schematic with anti-IL-34 antibody and control IgG. DAPI, blue.

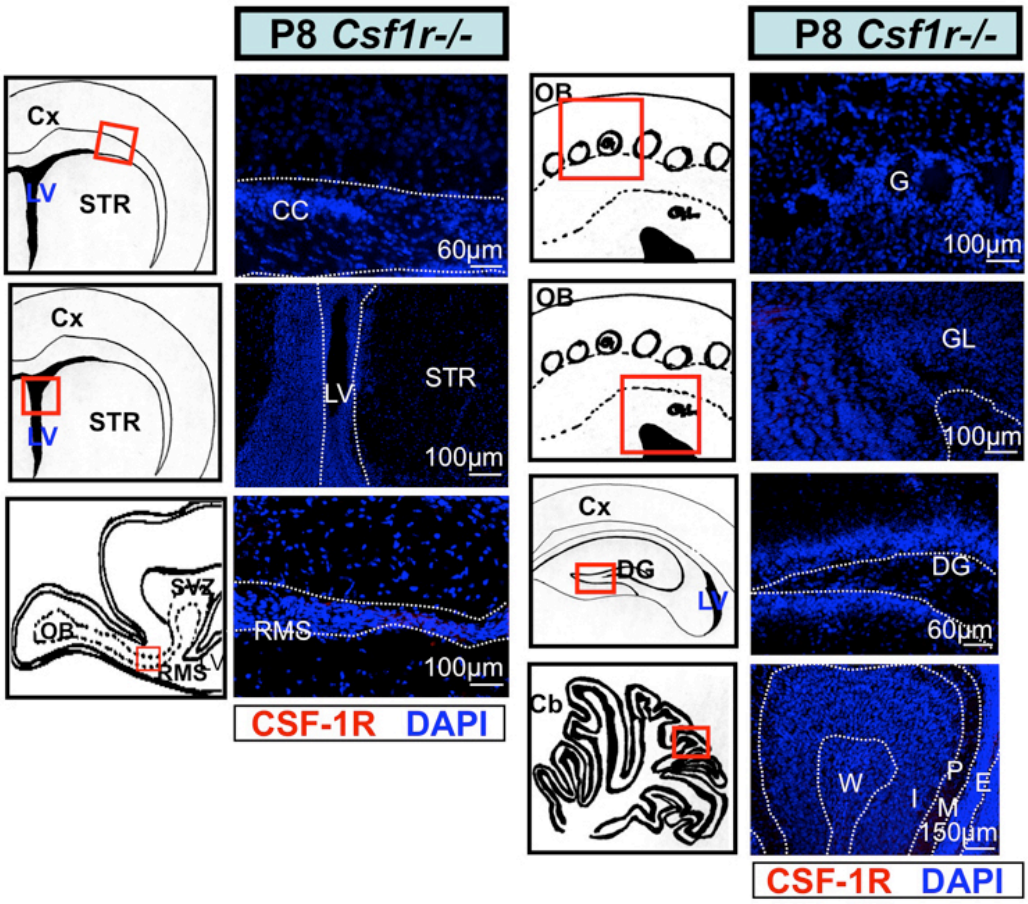

Fig. S3. Specificity of the anti-CSF-1R antibody. Absence of CSF-1R staining in various brain regions of P8 *Csf1r-/-* mice (counterstained with DAPI). Dotted lines delineate the contours of the structures. W, white matter; I, internal granular layer; P, Purkinje cell layer; M, molecular layer; E, external granular layer; Cx, cortex; OB, olfactory bulb; RMS, rostral migratory stream; DG, dentate gyrus; LV, lateral ventricle; Cb, cerebellum; CC, corpus callosum; G, glomerulus; GL, granular layer; STR, striatum; SVZ, subventricular zone.

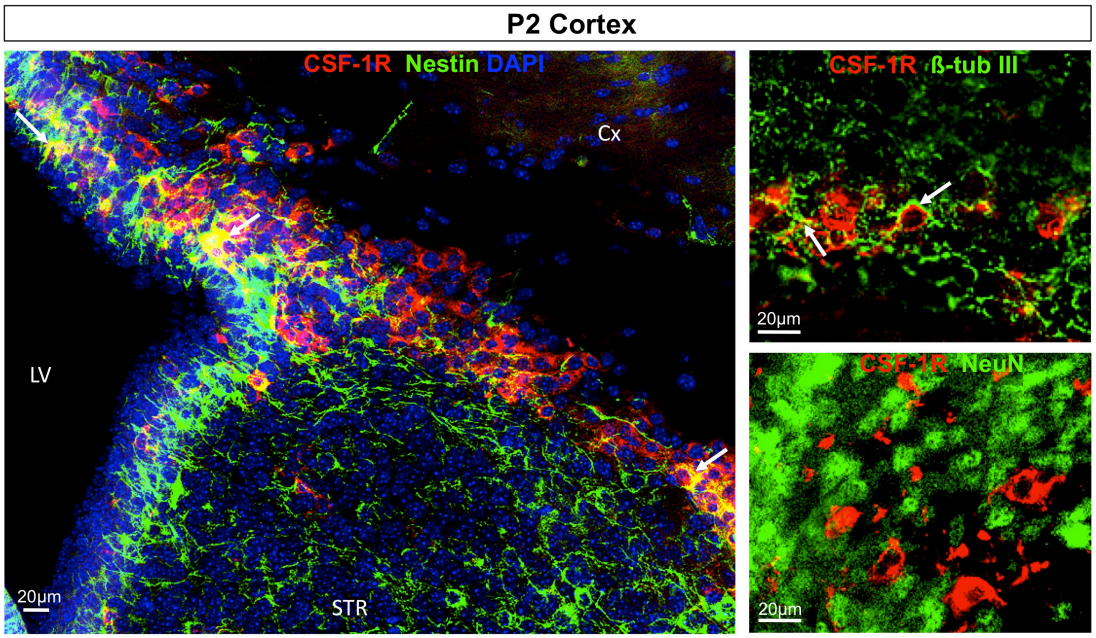

Fig. S4. CSF-1R expression on early postnatal dorsal forebrain neural progenitors and immature neurons. Immunostaining of P2 wild type brain sections reveal partial co-expression of CSF-1R (red) in Nestin (green) (left panel) and β-tub III (green) expressing cells (right top panel). Arrows indicate co-localization. Note the absence of CSF-1R (red) expression from NeuN (green) expressing mature neurons (right bottom panel). DAPI was used as a background in the left panel. Cx, cortex; LV, lateral ventricles; STR, striatum.

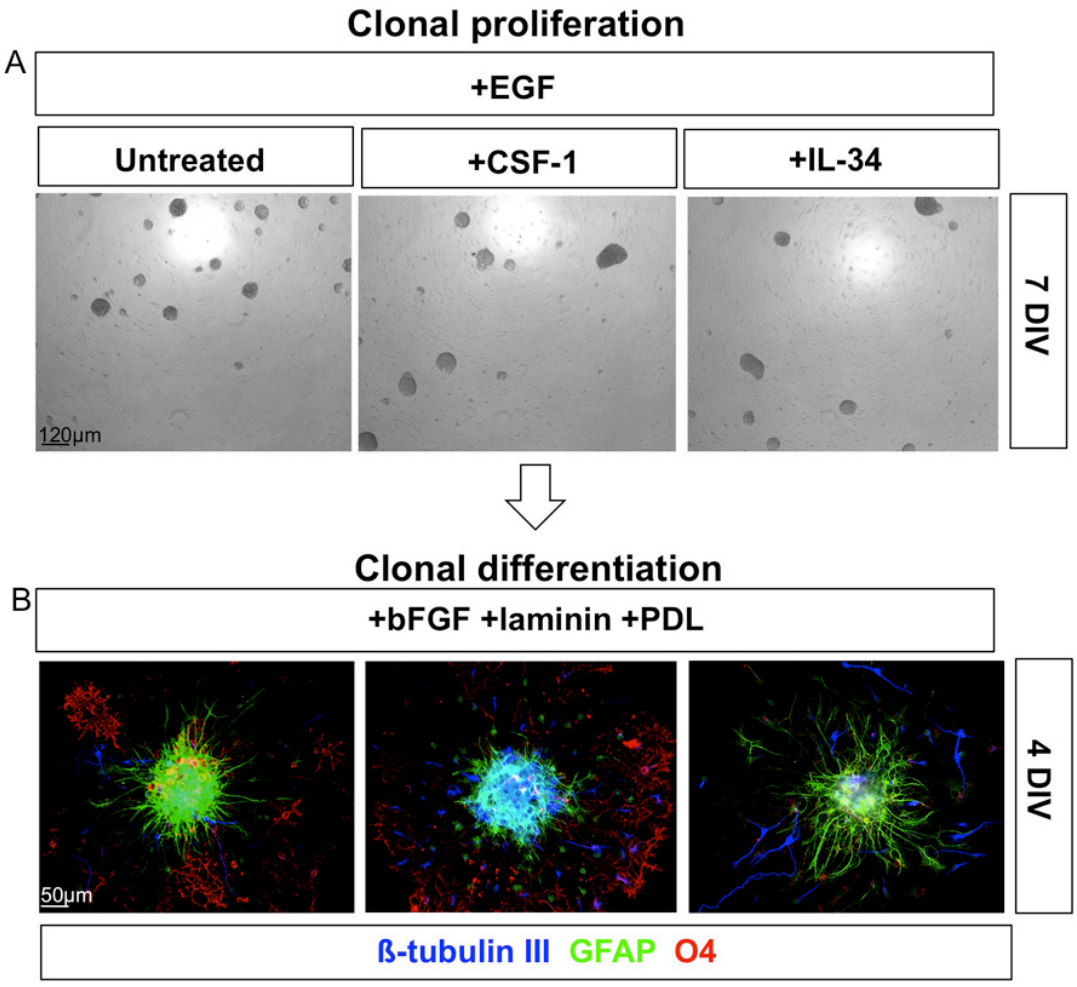

Fig. S5. Clones of proliferating or differentiating early postnatal dorsal forebrain progenitors. (A) Representative fields showing progenitor clones after culture for 7 DIV under the proliferation conditions, without or with CSF-1, or IL-34. Clonal sizes comparable to those with CSF-1 or IL-34 were obtained with CSF-1 plus IL-34 (data not shown). (B) Adherent clones, after culture under differentiation conditions for 4 DIV, were immunostained for neural lineage markers. Representative pictures of the most predominant differentiated clonal type for each of the treatments (untreated, CSF-1 or IL-34 treated) are shown. Note that treatment with CSF-1 or IL-34 generated more neurons (β-tub III+) and fewer astrocytes (GFAP+) in the multipotent clones and that IL-34 alone predominantly generated Neuron/Astrocyte bi-potent clones.

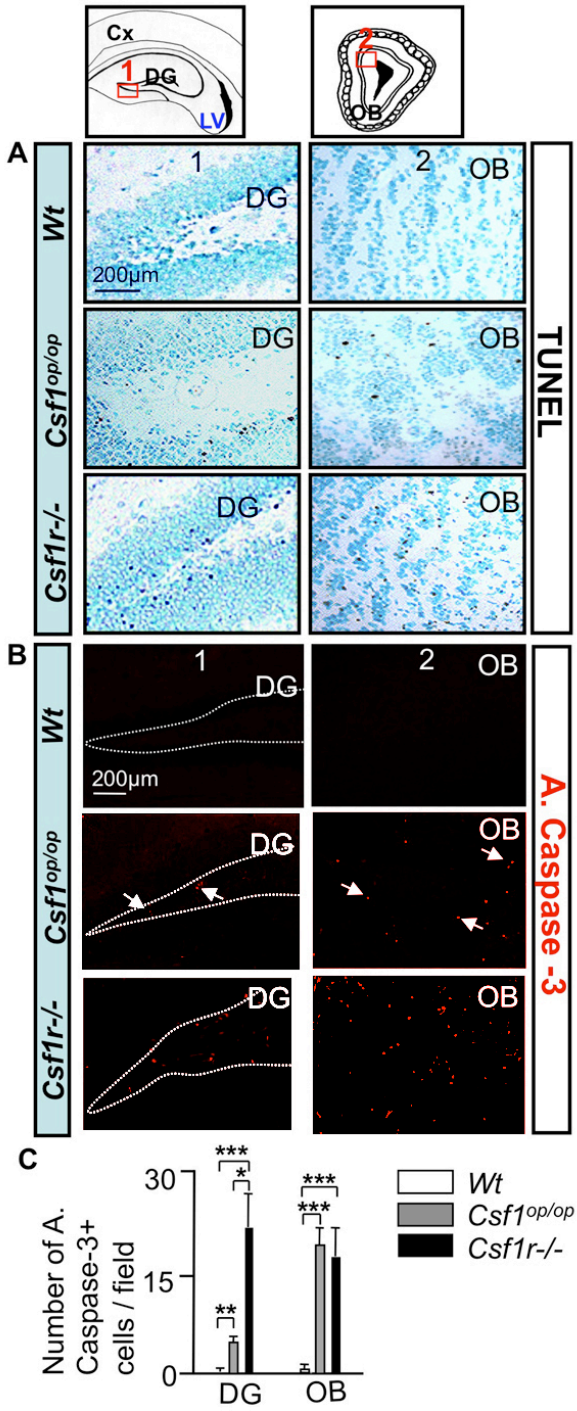

Fig. S6. *Csf1*$^{op/op}$ and *Csf1r-/-* brains have increased numbers of apoptotic cells in the areas associated with adult neurogenesis. Photomicrographs of (A) TUNEL+ (brown dots) and (B) active caspase-3+ (red dots) apoptotic cells in three-week-old *Wt* and mutant brains in the boxed regions of the schematics depicting DG and OB. Arrows in (B) indicate active caspase-3+ cells. Dotted lines delineate the contours of the inner lining of the granule layer. (C) Quantitation of the number of active caspase-3+ apoptotic cells/field. Averages of five different low-power (10X) fields per region per genotype; *, P<0.05; **, P<0.01 and ***, P<0.001.

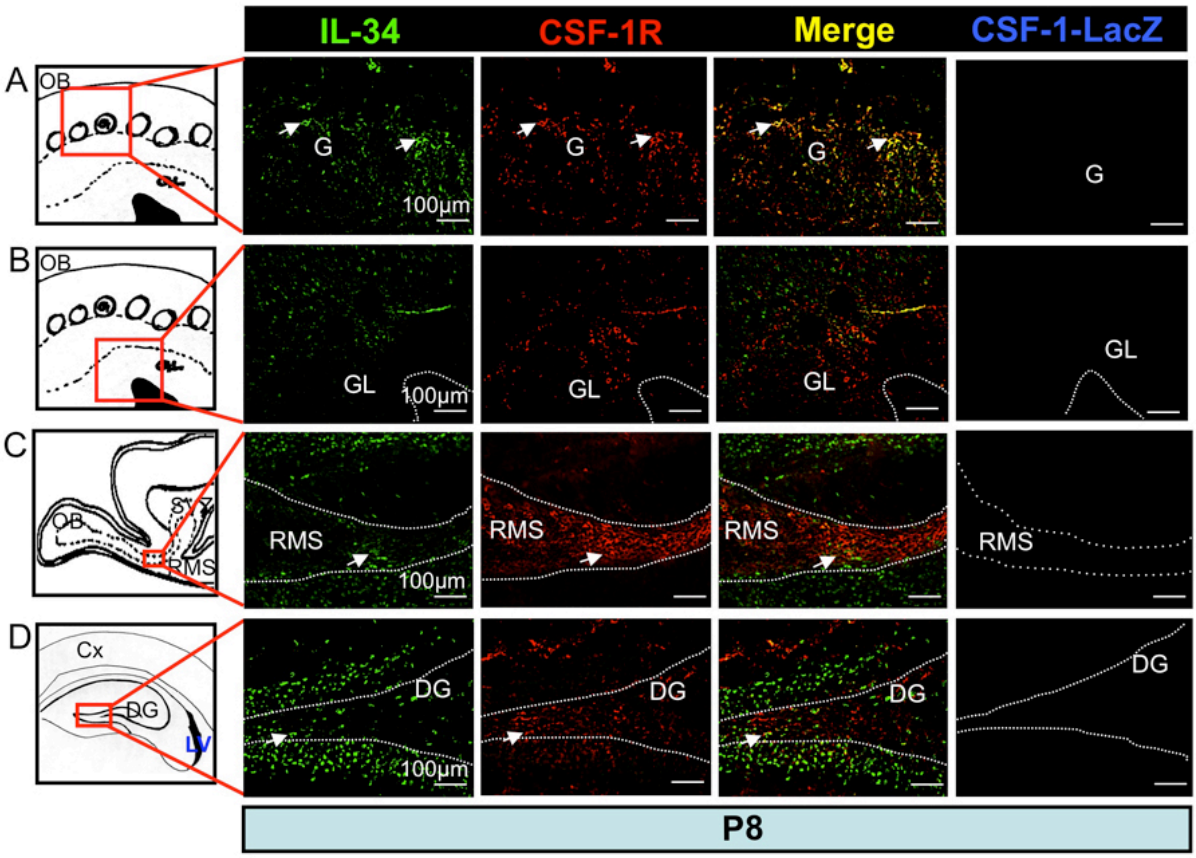

Fig. S7. The co-existence, with occasional co-expression, of IL-34 and CSF-1R in early postnatal forebrain regions, in the absence of CSF-1 expression. Immunostaining of P8 *TgZ* brain sections reveal expression of IL-34 (green) and CSF-1R (red) in the glomerular region (A) and the granule cell layer (B) of the OB, in the RMS (C) and in the DG (D). Arrows indicate co-localization. Note the absence of CSF-1 reporter (blue) expression in all of these regions. Dotted lines delineate the contours of the structures. OB, olfactory bulb; G, glomerulus; GL, granule cell layer; Cx, cortex; LV, lateral ventricles; DG, dentate gyrus; SVZ, subventricular zone; RMS, rostral migratory stream.

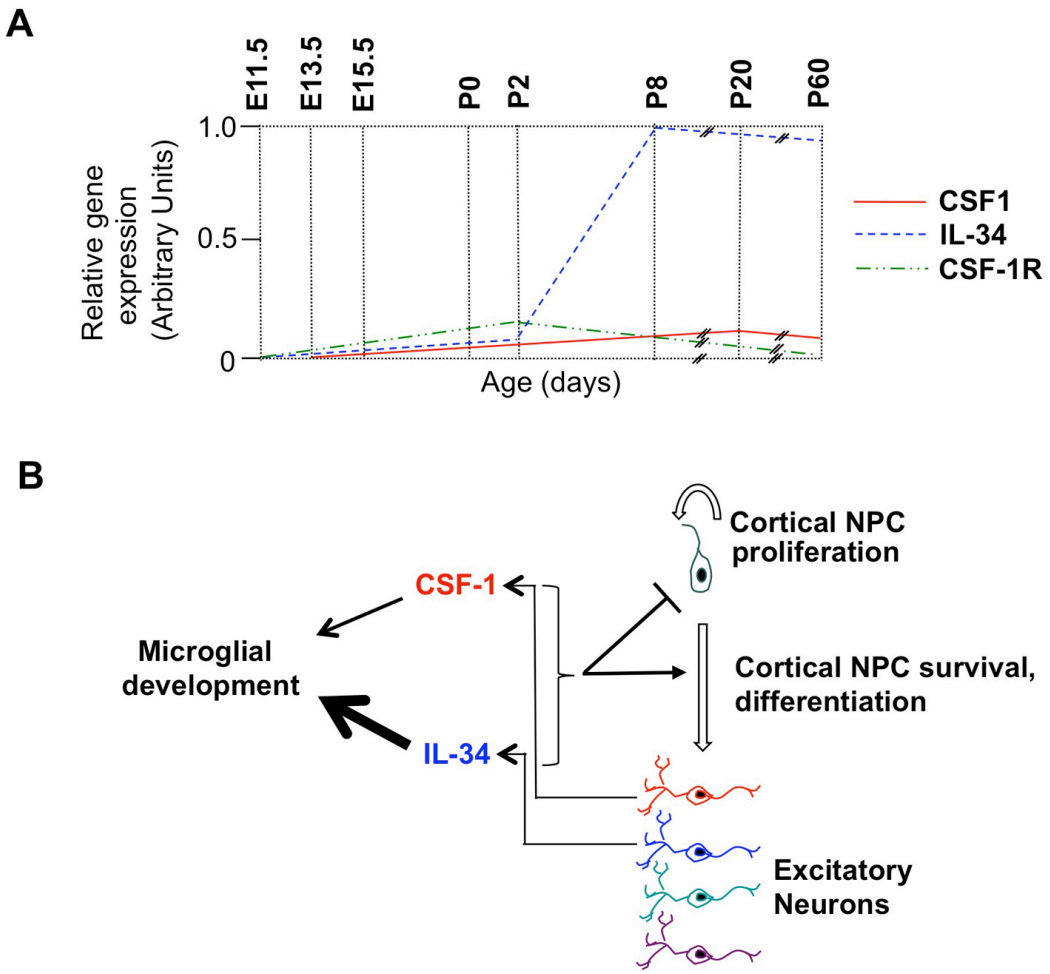

Fig. S8. Schemes. (A) Temporal patterns of CSF-1, IL-34 and CSF-1R expression during development. Y axis values at P8 and P60 are relative mRNA levels determined by real time QRT-PCR (also supported by IL-34, CSF-1 reporter and CSF-1R protein expression data). Y axis values for all other time points are solely based on relative protein expression (histochemistry or immunohistochemistry) or mRNA expression (in-situ hybridization, reporter gene expression) data. (B) Model of CSF-1R-signaling in brain based on analysis of the neocortex. Consistent with the more extensive expression of IL-34 compared with the expression of CSF-1, IL-34 is likely to play the major *in vivo* role in microglial development. Both CSF-1 and IL-34 inhibit neural progenitor cell (NPC) expansion, but promote NPC survival and facilitate NPC differentiation to neurons. Specific neuronal subsets express CSF-1 and IL-34.

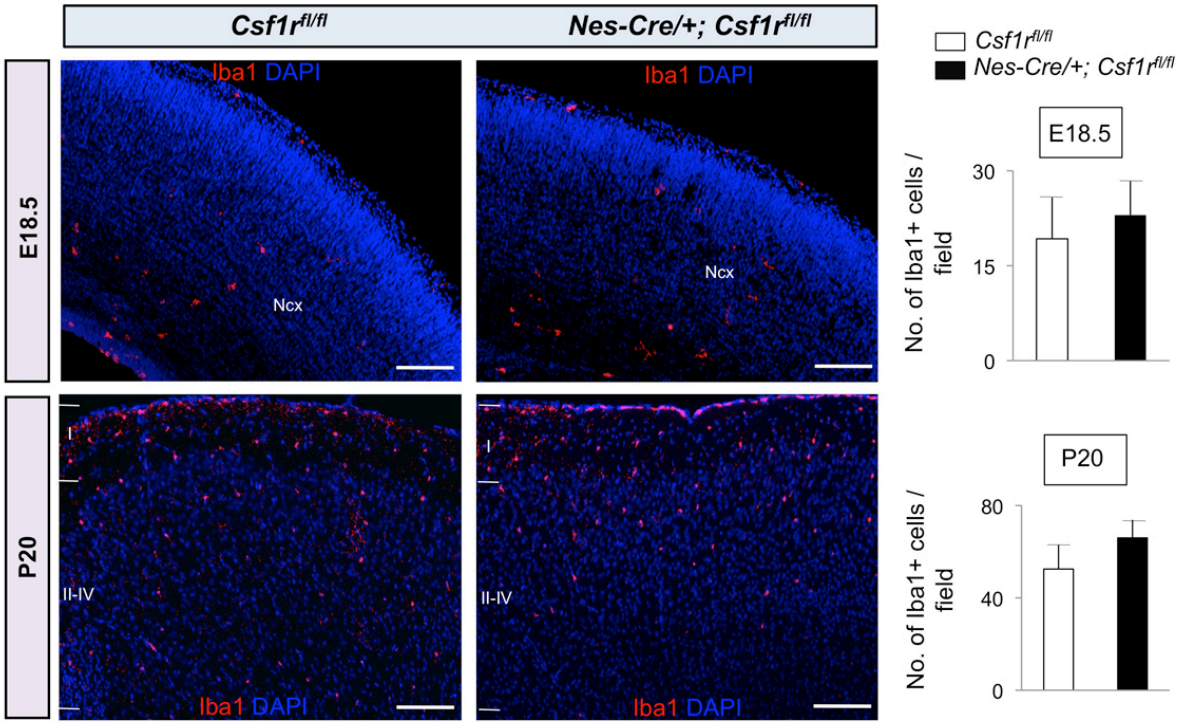

Fig. S9. Cortical microglial density is unaffected in *Nes-Cre/+; Csf1r*$^{fl/fl}$ mice. Neocortex from E18.5 (upper panels) and P20 (lower panels) mice, stained for microglia with anti-Iba1 antibody (red). Quantitation reveals no difference in microglial density, whether the *Csf1r* gene was conditionally deleted or not. Means ± SD of four different representative low-power (10X) fields per region per genotype from two different mice per genotype. Counterstained with DAPI. Bar, 150 μm. Ncx, neocortex. Lower panels show positions of cortical layers.

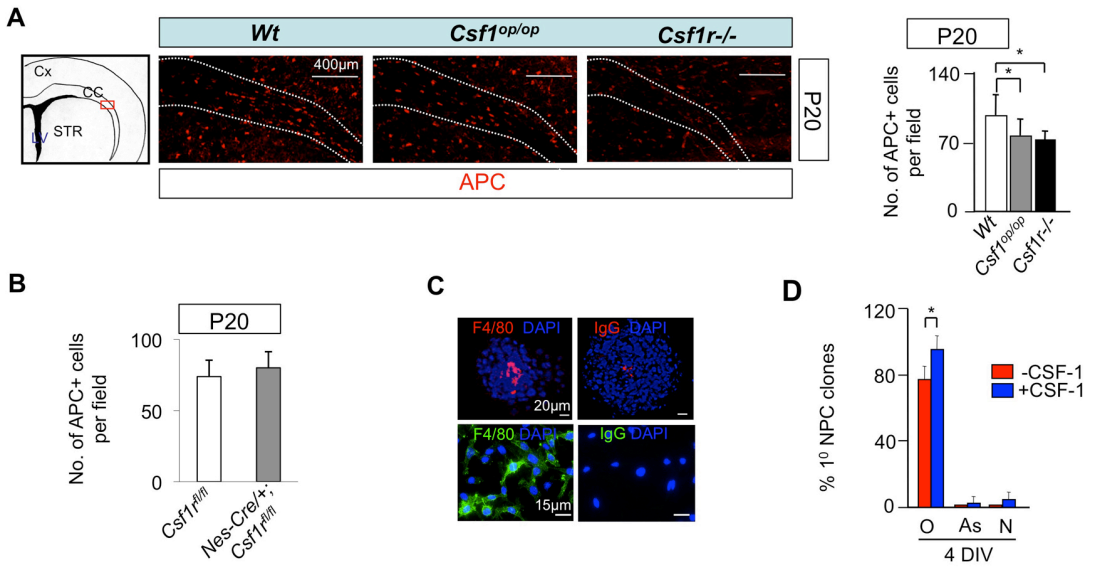

Fig. S10. CSF-1R, acting via microglia, facilitates oligodendrogliogenesis. (A,B) *In vivo* experiments: Immunofluorescence microscopy of coronal sections of (A) P20 *Wt*, *Csf1*$^{op/op}$ and *Csf1r-/-* cortical forebrain regions boxed in the diagram, showing APC+ mature oligodendrocytes. Dotted lines delineate the contours of the corpus callosum. Quantitation reveals a loss of mature oligodendrocytes in *Csf1*$^{op/op}$ and *Csf1r-/-* mutants, but (B) no change in their number in P20 *Nes-Cre/+; Csf1r*$^{fl/fl}$ mutants. (C,D) *In vitro* experiments: (C) Presence of microglia in colonies derived from unpurified early postnatal cortical progenitors. Left upper panel, Immunofluorescent F4/80 staining (red) of an adherent primary neural progenitor colony from cells plated after 7 days of suspension culture in EGF and cultured for an additional 4 days on poly-D-lysine-coated coverslips in the presence of laminin and bFGF. Right upper panel, another colony stained with control rat IgG (red), showing microglial contamination in these cultures. Left lower panel, F4/80 immunoreactivity (green) of BAC1.2F5 macrophages (as a positive control) with DAPI (blue) staining. Right lower panel, control rat IgG (green) staining of BAC1.2F5 cells, showing specificity of F4/80 antibody. (D) CSF-1 facilitates oligodendroglial differentiation of unpurified early postnatal cortical neural progenitors. Adherent clones generated in the presence of EGF and CSF-1 for 7 DIV and subsequently propagated under differentiation conditions as described in (C) for 4 DIV. Percentage of primary progenitor clones containing β tub-III+ neurons (N), GFAP+ astrocytes (As) and O4+ oligodendrocytes (O). Means ± SEM of 16 different representative fields from three independent experiments between untreated and CSF-1 treated conditions. *P<0.05.

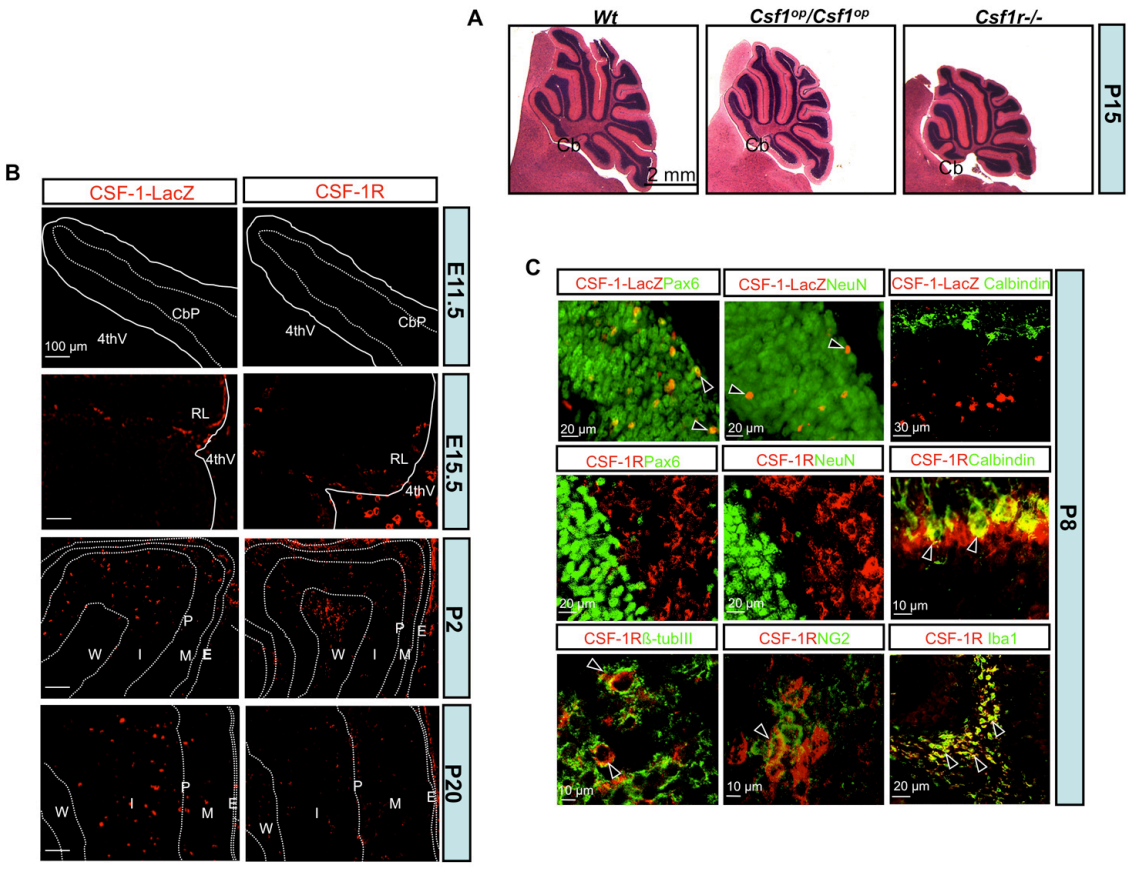

Fig. S11. CSF-1R-mediated cerebellar development. (A) Developmental abnormalities in P15 *Csf1*$^{op/op}$ and *Csf1r-/-* mice. H&E staining of mid-sagittal sections showing graded reduction in the cerebellar size from *Csf1*$^{op/op}$ to *Csf1r-/-* mice. (B) Spatio-temporal expression of the CSF-1-reporter and CSF-1R in *TgZ* cerebellum. Dotted lines delineate the contours of the structures. E11.5: Lack of CSF-1 reporter/CSF-1R expression in cerebellar primordium. E15.5: Expression of CSF-1 reporter/CSF-1R in the rhombic lip. P2: The CSF-1 reporter is expressed in the external and internal granule cell layers, whereas the CSF-1R is predominantly expressed in the Purkinje cell layer and white matter. Some CSF-1/CSF-1R expression is present in the molecular layer (the CSF-1R staining outside the external granule layer is non-specific). P20: CSF-1 reporter expression is similar to the staining observed at P2, whereas the CSF-1R expression pattern, although similar, is reduced. (C) Expression of the CSF-1 reporter and CSF-1R in P8 cerebellar cell types of *TgZ/+* mice. Confocal images showing CSF-1 reporter and CSF-1R (red) co-staining with granule cell markers, Pax6 (green) and NeuN (green), the Purkinje cell marker, calbindin (green), the molecular layer neuronal marker, ß-tub III (green) and the microglial markers, Iba1 (green) and NG2 (green) (Jones et al., 2002). Arrowheads indicate overlap of staining. W, white matter; I and E, internal and external granule cell layers; P, Purkinje cell layer; M, molecular layer, Cb, cerebellum; CbP, cerebellar primordium, RL, rhombic lip; 4th V, 4th ventricle.

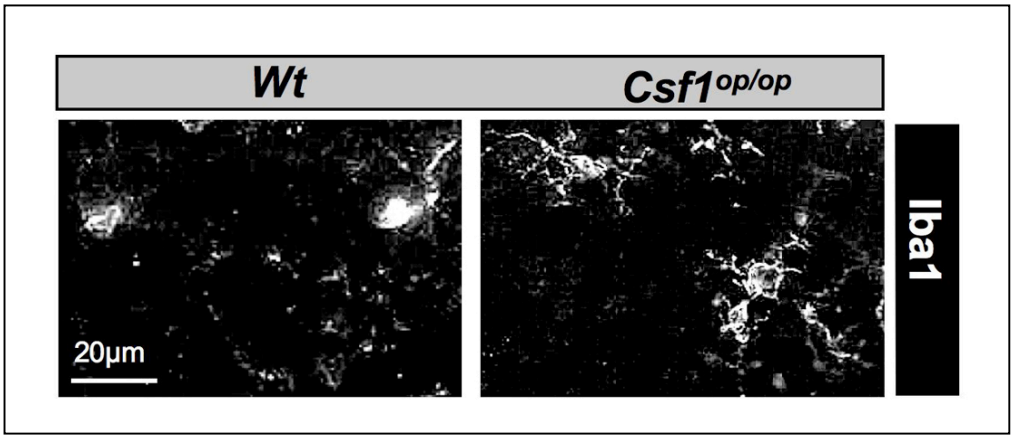

Fig. S12. Amoeboid microglia are rare in *Csf1*$^{op/op}$ brains. Iba1-staining of P20 brain sections reveal that in contrast to *Wt* brains, ramified, but not amoeboid microglia, are frequently present in *Csf1*$^{op/op}$ brains.

References

Dai, X. M., Zong, X. H., Sylvestre, V., Stanley, E. R., 2004. Incomplete restoration of colony-stimulating factor 1 (CSF-1) function in CSF-1-deficient Csf1op/Csf1op mice by transgenic expression of cell surface CSF-1. Blood. 103**,** 1114-23.

Hume, D. A., Robinson, A. P., MacPherson, G. G., Gordon, S., 1983. The mononuclear phagocyte system of the mouse defined by immunohistochemical localization of antigen F4/80. Relationship between macrophages, Langerhans cells, reticular cells, and dendritic cells in lymphoid and hematopoietic organs. J Exp Med. 158**,** 1522-36.

Jones, L. L., Yamaguchi, Y., Stallcup, W. B., Tuszynski, M. H., 2002. NG2 is a major chondroitin sulfate proteoglycan produced after spinal cord injury and is expressed by macrophages and oligodendrocyte progenitors. J Neurosci. 22**,** 2792-803.

Nandi, S., Akhter, M. P., Seifert, M. F., Dai, X. M., Stanley, E. R., 2006. Developmental and functional significance of the CSF-1 proteoglycan chondroitin sulfate chain. Blood. 107**,** 786-95.

Ryan, G. R., Dai, X. M., Dominguez, M. G., Tong, W., Chuan, F., Chisholm, O., Russell, R. G., Pollard, J. W., Stanley, E. R., 2001. Rescue of the colony-stimulating factor 1 (CSF-1)-nullizygous mouse (Csf1(op)/Csf1(op)) phenotype with a CSF-1 transgene and identification of sites of local CSF-1 synthesis. Blood. 98**,** 74-84.